

### Clinical characteristics and management of retinitis pigmentosa

Nguven, X.T.

#### Citation

Nguyen, X. T. (2024, January 23). *Clinical characteristics and management of retinitis pigmentosa*. Retrieved from https://hdl.handle.net/1887/3714325

Version: Publisher's Version

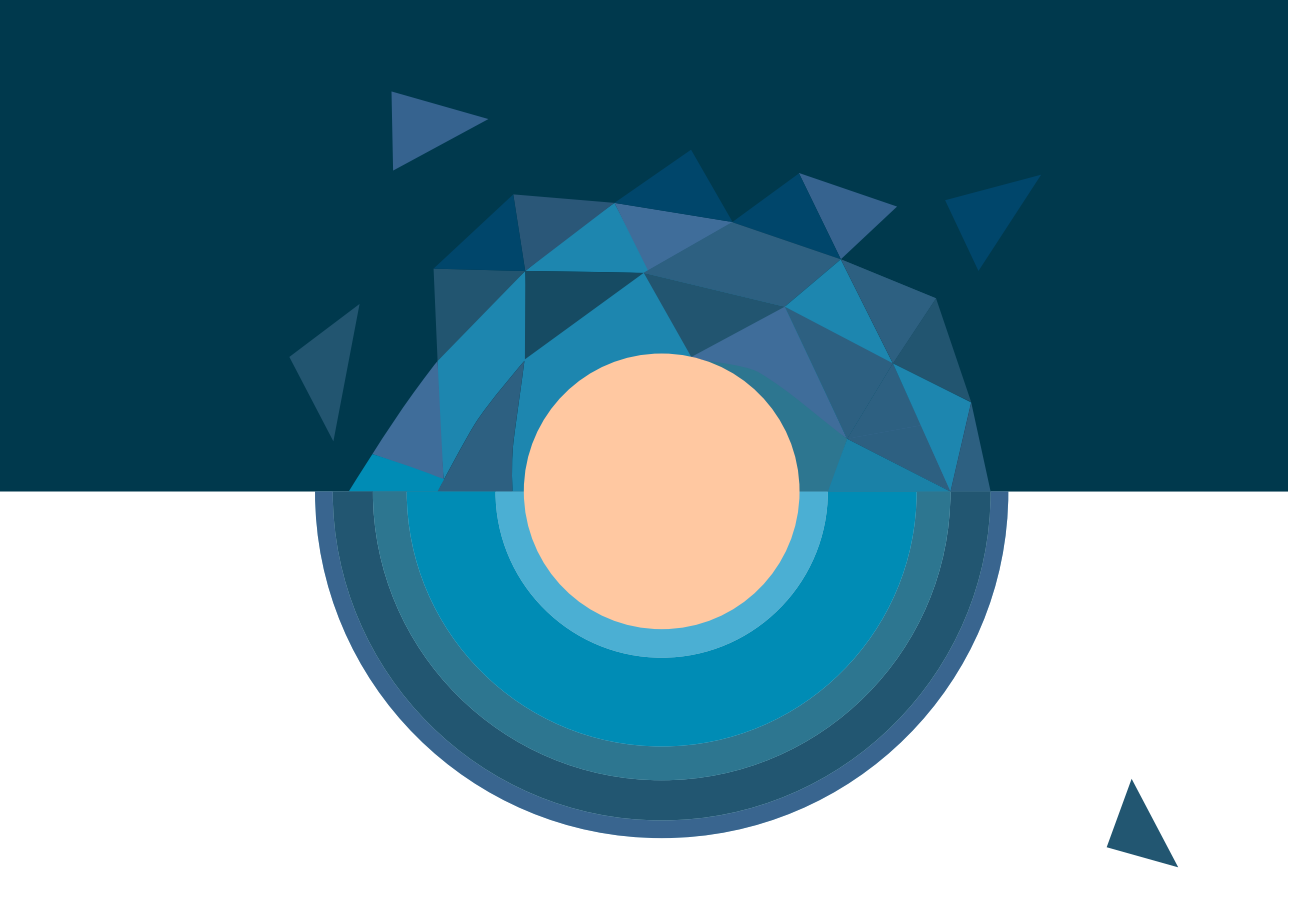
Licence agreement concerning inclusion of doctoral

License: thesis in the Institutional Repository of the University

of Leiden

Downloaded from: <a href="https://hdl.handle.net/1887/3714325">https://hdl.handle.net/1887/3714325</a>

**Note:** To cite this publication please use the final published version (if applicable).



# **PART I**

CLINICAL CHARACTERISTICS AND NATURAL HISTORY STUDIES





### **CHAPTER 2.1**

## CLINICAL CHARACTERISTICS AND NATURAL HISTORY OF RHO-ASSOCIATED RETINITIS PIGMENTOSA: A LONG-TERM FOLLOW-UP STUDY

Xuan-Thanh-An Nguyen<sup>1</sup>, Mays Talib <sup>1\*</sup>, Caroline van Cauwenbergh<sup>2</sup>, Mary J. van Schooneveld<sup>3</sup>, Marta Fiocco <sup>4,5</sup>, Jan Wijnholds<sup>1</sup>, Jacoline B. Ten Brink<sup>6</sup>, Ralph J. Florijn<sup>6</sup>, Nicoline E. Schalij-Delfos<sup>1</sup>, Gislin Dagnelie<sup>7</sup>, Maria M. van Gederen<sup>8,9</sup>, Elfride de Baere<sup>2</sup>, Magda A. Meester-Smoor<sup>10</sup>, Julie De Zaeytijd<sup>2</sup>, Irina Balikova<sup>2</sup>, Alberta A. Thiadens<sup>10</sup>, Carel B. Hoyng<sup>11</sup>, Caroline C. Klaver<sup>10,11,12</sup>, L. Ingeborgh van den Born<sup>13</sup>, Arthur A. Bergen<sup>6,14</sup>, Bart P. Leroy<sup>2,15</sup>, and Camiel J. F. Boon<sup>1,3</sup>

Retina. 2021;41(1):213-223



<sup>&</sup>lt;sup>1</sup> Department of Ophthalmology, Leiden University Medical Center, Leiden, The Netherlands.

<sup>&</sup>lt;sup>2</sup> Department of Ophthalmology, Ghent University and Ghent University Hospital, Ghent, Belgium.

<sup>&</sup>lt;sup>3</sup> Department of Ophthalmology, Amsterdam UMC, Academic Medical Center, Amsterdam, The Netherlands.

<sup>&</sup>lt;sup>4</sup>Institute of Mathematic Leiden University, Leiden, The Netherlands.

<sup>&</sup>lt;sup>5</sup> Department of Biomedical Data Sciences, Leiden University Medical Center, Leiden, The Netherlands.

<sup>&</sup>lt;sup>6</sup> Department of Clinical Genetics, Amsterdam UMC, Academic Medical Center, Amsterdam, The Netherlands.

<sup>&</sup>lt;sup>7</sup> Wilmer Eye Institute, Johns Hopkins University, Baltimore, Maryland.

<sup>&</sup>lt;sup>8</sup> Bartiméus, Diagnostic Centre for Complex Visual Disorders, Zeist, The Netherlands.

<sup>&</sup>lt;sup>9</sup>Department of Ophthalmology, University Medical Center Utrecht, Utrecht, The Netherlands.

<sup>&</sup>lt;sup>10</sup> Department of Ophthalmology, Erasmus Medical Center, Rotterdam, The Netherlands.

Department of Ophthalmology, Radboud University Medical Center, Nijmegen, The Netherlands.

<sup>&</sup>lt;sup>12</sup> Department of Epidemiology, Erasmus Medical Center, Rotterdam, The Netherlands.

<sup>&</sup>lt;sup>13</sup> The Rotterdam Eye Hospital, Rotterdam, The Netherlands.

<sup>&</sup>lt;sup>14</sup> The Netherlands Institute for Neuroscience (NIN-KNAW), Amsterdam, The Netherlands; and.

<sup>&</sup>lt;sup>15</sup> Ophthalmic Genetics & Visual Electrophysiology, Division of Ophthalmology, the Children's Hospital of Philadelphia Philadelphia, Pennsylvania.

<sup>\*</sup>Joint first authors.

#### **ABSTRACT**

#### **Purpose**

To investigate the natural history of RHO-associated retinitis pigmentosa (RP).

#### Methods

A multicenter, medical chart review of 100 patients with autosomal-dominant *RHO*-associated RP.

#### Results

Based on visual fields, time-to-event analysis revealed median ages of 52 and 79 years to reach low vision (central visual field <20°) and blindness (central visual field <10°), respectively. For best-corrected visual acuity (BCVA), the median age to reach mild impairment (20/67  $\leq$  BCVA <20/40) was 72 years, whereas this could not be computed for lower acuities. Disease progression was significantly faster in patients with a generalized RP phenotype (n = 75; 75%) compared to patients with a sector RP phenotype (n = 25; 25%), in terms of decline rates of BCVA (p < 0.001), and V4e retinal seeing areas (p < 0.005). The foveal thickness of the photoreceptor-retinal pigment epithelium (PR+RPE) complex correlated significantly with BCVA (Spearman's  $\rho$ =0.733; p < 0.001).

#### **Conclusions**

Based on central visual fields, the optimal window of intervention for *RHO*-associated RP is before the 5<sup>th</sup> decade of life. Significant differences in disease progression are present between generalized and sector RP phenotypes. Our findings suggest that the PR+RPE complex is a potential surrogate endpoint for BCVA in future studies.

#### INTRODUCTION

Mutations in the *RHO* gene are associated with the autosomal-dominant form of retinitis pigmentosa (RP).<sup>1</sup> Initial symptoms of RP include night blindness or peripheral visual field loss, which can be followed by loss of central vision in advanced stages of disease. To date, over 150 mutations in the *RHO* gene have been described, which are responsible for 25-30% of all autosomal-dominant retinitis pigmentosa (adRP) cases.<sup>2</sup> *RHO* mutations have also been described in congenital stationary night blindness,<sup>3</sup> and even more rarely, in forms of autosomal-recessive RP.<sup>4</sup> Another phenotype commonly described in *RHO* mutations is sector RP, which is characterized by regional photoreceptor degeneration, typically confined to the inferior quadrant of the retina.<sup>5,6</sup> Sector RP is considered a stationary to slowly progressive disease, but may eventually lead to a more severe, diffuse RP phenotype.<sup>7</sup>

The *RHO* gene encodes the protein rhodopsin, located in the outer segment of rod photoreceptor cells, containing extracellular, transmembrane, and cytoplasmic domains.¹ Previous studies have shown that the clinical expression of *RHO*-associated RP correlates with the protein domain affected by the mutation.<sup>8</sup> Mutations affecting the cytoplasmic domain of rhodopsin are more likely to cause a severe RP phenotype, with early loss of rod and cone function. In contrast, patients with mutations affecting the extracellular domain generally have a milder phenotype, with relatively preserved rod and cone function, and slower disease progression.<sup>9, 10</sup>

No curative treatment for *RHO*-associated RP is currently available, but promising results have been achieved by knockdown-and-replacement gene therapy in animal models.<sup>11, 12</sup> To guide the design of upcoming clinical trials, more insight into the natural disease progression in *RHO*-associated RP is necessary. A more detailed clinical disease profile will aid in the selection of eligible candidates, and the establishment of appropriate clinical endpoints for future trials. The purpose of this longitudinal study was to provide a description of the clinical variability and the natural disease course in patients with *RHO*-associated RP in a large cohort.

#### MATERIALS AND METHODS

#### Study population

Patients with *RHO*-associated RP were collected from the patient database for hereditary eye diseases (Delleman Archive) at the Amsterdam University Medical Centers (The Netherlands), from various other Dutch tertiary referral centers within the RD5000 consortium,<sup>13</sup> and from Ghent University Hospital in Belgium. Inclusion criteria were: a molecular confirmation of a (likely) pathogenic variant in the *RHO* gene, or a first-degree relative with similar clinical findings and molecular

confirmation of a *RHO* mutation. In total, 100 patients with *RHO*-associated RP were included for analysis in this study. Approval from the Ethics Committee was obtained prior to the study, as well as local Institutional Review Board approval in all participating centers. Dutch participants provided informed consent for the use of their patient data for research purposes. For Belgian subjects, the local Ethics Committee waivered the need for informed consent on the condition of pseudonymization.

#### Data collection

A standardized review of medical records was performed for data on the initial symptoms, best-corrected visual acuity (BCVA), findings on slit-lamp examination and fundoscopy, Goldmann visual fields (GVF), full-field electroretinogram (ERG), spectral-domain optical coherence tomography (SD-OCT), and fundus autofluorescence (FAF) imaging, where available. GVFs were digitized and converted to retinal seeing areas using methods previously described by Dagnelie.<sup>14</sup>

In patients with available OCT and FAF imaging in Heidelberg (Heidelberg Engineering, Heidelberg, Germany), automatic and manual measurement of retinal layers were performed using the inbuilt software of Heidelberg. The thickness of the photoreceptor-retinal pigment epithelium complex (PR+RPE), was defined as the foveal distance between the external limiting membrane and the basal border of the retinal pigment epithelium, as described previously (see Figure, Supplemental Digital Content 1).<sup>15</sup> All measurements were performed by two authors (XN and MT), and reviewed by CJFB in case of inconsistency between the aforementioned two authors.

#### Statistical analysis

Data were analyzed using SPSS version 23.0 (IBM Corp. Armonk, NY, USA) and the R-software environment.<sup>16</sup> Findings with a p-value of <0.05 were considered statistically significant. Normally and non-normally distributed data were displayed as means with standard deviations (SD), and medians with interquartile ranges (IQR), respectively. To measure the time to visual impairment, a time-to-event analysis was performed using the nonparametric maximum likelihood estimator (NPMLE) method to account for left, interval and right censored data. Visual impairment endpoints were based on the criteria of the World Health Organization: No visual impairment (BCVA ≥ 20/40), mild visual impairment (20/67  $\leq$  BCVA < 20/40), low vision (20/200  $\leq$  BCVA < 20/67), severe visual impairment (20/400 ≤ BCVA < 20/200) or blindness (BCVA < 20/400). For visual fields, the following endpoints were used: mild impairment ( $20^{\circ} \le \text{central visual field} < 70^{\circ}$ ), low vision (central visual field < 20°) and blindness (central visual field < 10°). Due to the presence of repeated measurements, a linear mixed model analysis was performed to measure disease progression. For hand movement vision, light perception vision and no light perception, logMAR values of 2.7, 2.8 and 2.9 were used, respectively.<sup>17</sup> Structurefunction correlations were analyzed using Spearman correlation coefficients. To analyze

genotype-phenotype associations, patients were stratified into 3 groups, based the affected protein domain: cytoplasmic, transmembrane or extracellular.

#### **RESULTS**

#### Clinical and genetic characteristics

One-hundred patients from 47 families, with autosomal dominant *RHO* mutations, were included from the Dutch (n=63; 63%) and Belgian (n=37; 37%) population. No differences in baseline characteristics between these two populations were present (see Table, Supplemental Digital Content S2). Patients with available longitudinal data (n=72; 72%) had a median follow-up time of 6.9 years (IQR 11.9; range: 0.2-41.0) and a median of 5.0 visits (IQR 6.0, range: 2.0 – 31.0). Seventy-five patients (75%) had a generalized form of RP on fundus examination (Figure 1), whereas 25 patients (25%) showed a sector RP phenotype, with pigmentary changes confined to the inferior hemisphere in all cases. The clinical characteristics of the entire cohort are summarized in Table 1.

In total, 23 different missense mutations, 1 in-frame deletion, and 1 novel splice site mutation were found in the *RHO* gene (see Table, Supplemental Digital Content S3). Patients were stratified, based on the affected protein domain, as carrying extracellular (n=64; 64%), transmembrane (n=20; 20%), or cytoplasmic (n=15; 16%) mutations, excluding the splice site mutation. We found a high proportion of extracellular mutations (24/25; 96%) in the sector RP group. The most common pathogenic variant in this study, p.(Glu181Lys), was found in 4 families, comprising 23 out of the 63 Dutch patients (37%). This mutation was not found in the Belgian cohort. Common mutations exclusively found in the Belgian cohort were p.(Ile255del) (n=6) and p.(Tyr178Asp) (n=6), each belonging to a single family, accounting for 12 out of the 37 Belgian patients (32%).

**Table 1.** Characteristics of patients with RHO-associated (sector) retinitis pigmentosa at last examination.

Characteristics	Total	Generalized RP	Sector RP	P-value
	(n=100)	(n=75)	(n=25)	
Male (%)	44 (44)	34 (46)	10 (39)	0.642
Age at last examination (n=100)				
Mean ± SD	$43.5 \pm 18.5$	$42.5 \pm 19.3$	$45.5 \pm 22.6$	0.204
Initial symptoms (n=55)				
Nyctalopia, n (%)	41 (75)	28 (74)	2 (40)	
Visual field loss, n (%)	5 (9)	3 (8)	1 (20)	
Visual acuity loss, n (%)	3 (5)	2 (5)	1 (20)	
Multiple symptoms, n (%)	6 (11)	5 (13)	1 (20)	0.890‡
Age at onset in years (n=55)				
Early childhood, n (%)	21 (38)	16 (29)	5 (9)	
Median age (IQR)	13.5 (12.5)	11.0 (11.8)	15.7 (12.5)	0.829

**Table 1.** Characteristics of patients with RHO-associated (sector) retinitis pigmentosa at last examination. (continued)

Characteristics	Total (n=100)	Generalized RP (n=75)	Sector RP (n=25)	P-value
Mean refractive error, in D (n=66)	(11-100)	(11–73)	(11-23)	
Mean ± SD	0.8 ±2.85	1.0 ± 3.27	0.2 ± 1.4	0.298
BCVA in the better seeing eye (n=95)				
Median BCVA, in Snellen (IQR)	20/25 (20/30)	20/30 (20/30)	20/20 (20/200)	<0.001
BCVA in the worst seeing eye (n=95)				
Median BCVA, in Snellen (IQR)	20/30 (20/25)	20/33 (20/30)	20/22 (20/60)	0.002
Electroretinography patterns (n=52)		, , , ,	(,	
Normal responses, n (%)	2 (4)	_	2 (11)	
Reduced responses, n (%) †	5 (10)	1 (3)	4 (22)	
Rod-cone patterns, n (%)	28 (54)	16 (47)	12 (67)	
Minimal responses, n (%)	6 (11)	6 (18)	-	
Non-detectable, n (%)	11 (21)	11 (32)	-	<0.001‡
Retinal seeing areas, V4e (n=57)*	. ,	\- <i>,</i>		
Median seeing areas, in mm <sup>2</sup>	256.4 (545.6)	128.0 (552.4)	487.2 (248.3)	0.067
(IQR)				
Retinal seeing areas, I4e (n=55)*				
Median seeing areas, in mm <sup>2</sup>	17.4 (101.4)	14.5 (66.5)	130.6 (194.36)	0.011
(IQR)				
Visual field patterns (n=75)				
Normal, n (%)	1 (1)	1 (2)	_	
Peripheral constriction, n (%)	24 (32)	19 (32)	5 (31)	
Midperipheral scotoma, n(%)	6 (8)	5 (9)	1 (6)	
Central island with peripheral	18 (24)	15 (25)	3 (19)	
remnants, n (%)				
Central preservation, n (%)	19 (25)	18 (30)	1 (6)	
Superior hemisphere, n (%)	7 (10)	1 (2)	6 (38)	0.002‡
Cystoid macular edema, n (%)	16/32 (50)	14/25 (56)	2/7 (29)	0.225‡
Central retinal thickness (n=32)*				
Median thickness in μm (IQR)	253.0 (94.0)	254.0 (122.0)	248.5 (92.5)	0.858
Outer nuclear layer thickness				
(n=32)*				
Median thickness in $\mu m$ (IQR)	97.5 (47.25)	89.5 (52.5)	110.5 (41.9)	0.121
PR+RPE thickness (n=32)*				
Median thickness in μm (IQR)	90.5 (18.3)	89.5 (20.0)	95.3 (18.1)	0.147
Ellipsoid zone band width (n= 26)*				
Mean width in $\mu m \pm SD$	2704.5 ± 1881.9	2125.0 ± 1544.8	4277.5 ± 1909.6	0.007
Hyper-AF ring diameter (n=15)*				
Horizontal border in $\mu m \pm SD$	3541.6 ± 1930.6	3484.9 ± 2058.5	3910.3 ± 1009.4	0.571
Vertical border in $\mu m \pm SD$	2652.7 ± 1567.7	2594.9 ± 1628.0	3201.5 ± 883.2	0.286

Significant p values (p<0.05) are indicated in bold. The last available examination was used for documentation. RP, retinitis pigmentosa; SD, standard deviation; D, diopters; IQR, interquartile range; PR+RPE, photoreceptor-retinal pigment epithelium; hyper-AF, hyperautofluorescent. \*Averaged between eyes.  $\dagger$  No clear rod or cone response was documented.  $\ddagger$  Fisher's exact test was performed.

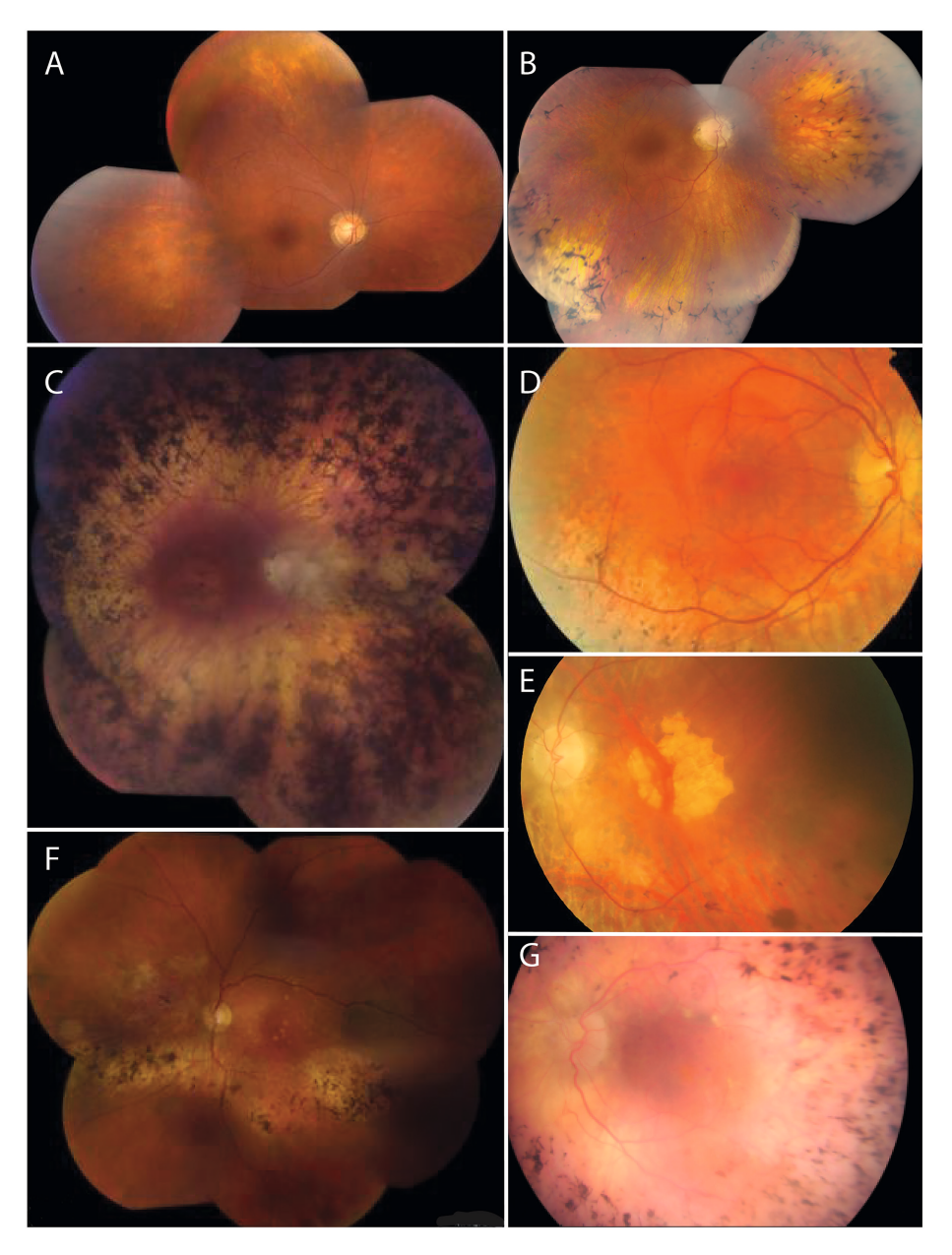


**Figure 1.** Colour fundus photography in this cohort of *RHO*-associated retinitis pigmentosa (RP). A-C, Illustrations of interfamilial and intrafamilial variability fundus in a family with p.(Tyr178Asn) mutations in the *RHO* gene. A, Patient-ID 65, aged 38, with mutation p.(Tyr178Asn). Peripapillary atrophy and moderate peripheral chorioretinal atrophy was present on fundus photography. No intraretinal hyperpigmentation was seen (best-corrected visual acuity [BCVA]: 20/20 in both eyes). B, Patient-ID 66, aged 45 years, with *RHO* mutation p.(Tyr178Asn). Fundus photography showed chorioretinal atrophy and bone-spicule hyperpigmentation in the midperiphery (BCVA right eye: 20/25; BCVA left eye: 20/67). C, Patient-ID 63, aged 50

years, carrying a p.(Tyr178Asn) in *RHO*. Fundus photography revealed optic disc pallor, attenuated vessels, ring-shaped atrophy in the macula and diffuse intraretinal bone-spicule hyperpigmentations (BCVA was 20/400 in both eyes). D, Patient-ID 52, aged 45 years, with *RHO* mutation p.(Glu28His). A sectorial RP phenotype is seen on colour fundus photography of the right eye, with peripapillary atrophy, and atrophic areas and bone spicule hyperpigmentation around the inferior vascular arcade (BCVA: 20/20 in both eyes). E, Patient-ID 51, aged 87 years, with *RHO* mutation p.(Leu40Pro). Fundus photography showed mild optic disc pallor with retinal atrophy following the superior and inferior vascular arcade. Geographic atrophy is visible at the macula of the left eye, resulting in a BCVA of only light perception. F, Patient-ID 80, aged 74 years, carrying a p.(Asn15Ser) mutation in *RHO*. Fundus photography of the left eye revealed paravascular atrophy mainly in the inferior quadrant with pigment clumping around these atrophic areas. Drusen can be seen around the macula (BCVA right eye: 20/22; BCVA left eye: 20/67). G, Patient-ID 48, aged 74 years, with the p.(Asp190Gly) *RHO* mutation, showing advanced RP. A pale fundus with a waxy pale optic disc, severely attenuated vessels, cystoid macular edema and bone-spicule hyperpigmentation in the midperipheral retina (BCVA right eye: 20/667; BCVA left eye: 20/1000).

#### Visual function

BCVA data were available for 95 patients, with a high degree of symmetry between eyes (Spearman's  $\rho = 0.888$ ; p < 0.001). In 25 patients, a degree of BCVA-based visual impairment was present during the last examination (see Figure, Supplemental Digital Content 4). Time-to-event analysis of the entire cohort revealed a median age of 72 years to reach mild visual impairment, while the median ages for low vision, severe and blindness could not be computed (Figure 2). First occurrences of low vision were seen from the 3th decade of life onwards, whereas severe visual impairment and blindness were seen from the 5th decade of life onwards. In the sector RP cohort, the first occurrence of blindness was seen after the 8th decade of life in a patient with agerelated macular degeneration. Linear mixed-model analysis revealed an age effect on mean BCVA, which was 0.012 logMAR (-2.9%; p < 0.001) per year for the entire cohort. BCVA decline was significantly faster in patients with a generalized RP phenotype than in patients with a sector RP phenotype (p = 0.002), with BCVA progression rates of 0.012  $\log$ MAR (-3.8%; p < 0.001) and -0.002  $\log$ MAR (+0.4%; p = 0.671) per year, respectively. For generalized RP patients, we found no differences in baseline BCVA values (p=0.360) or in progression slopes (p = 0.168) between affected protein domains.

Initial ERG findings were documented in 52 patients (Table 1). Minimal and non-detectable ERG responses were only found in the generalized RP group. The mean age at which non-detectable ERG responses were first observed was 35.3 years (SD 16.1; range 17.1-63.7). Longitudinal ERG data were available for 10 patients, with a mean follow-up time of 6.7 years (SD 4.0; range 0.5-13.6). Eight patients showed no clear changes in ERG-patterns during follow-up. Two patients, aged 29 and 26, displayed rod-cone patterns at the initial visit, which progressed to minimal and absent responses over a time span of 8.6 and 13.6 years, respectively.

Original GVF records were available for 59 patients, with high degree of symmetry between eyes for the V4e (Spearman's  $\rho = 0.957$ ; p < 0.001), and the I4e (Spearman's  $\rho = 0.935$ ; p < 0.001) retinal seeing areas. Various patterns of visual field defects were

observed, ranging from mild concentric constriction to central islands (Figure 3). Intrafamilial variability was present, as patients carrying the p.(Glu181Lys) mutation could demonstrate different visual field defects (Figure 3A-B). Time-to-event analysis of the visual fields revealed median ages of 44, 52 and 79 years for mild visual impairment, low vision and blindness, respectively (Figure 1B). For the V4e seeing areas, a faster decline of retinal seeing areas was observed in generalized RP patients compared to sector RP patients (p = 0.005), with a significant decline rate of -5.6% per year (p < 0.001) for generalized RP patients, but not in sector RP ( $\pm$ 1.7% per year, p = 0.477). No differences in V4e seeing areas were seen between domains at baseline (p = 0.240). nor with increasing age (p = 0.085) in generalized RP patients. For the I4e seeing areas. we found the age effect to be -5.5% per year (p < 0.001) in generalized RP patients. and +0.2% per year (p = 0.930) in sector RP patients. For generalized RP patients, we found differences at baseline (p = 0.013), with larger 14e seeing areas in patients with extracellular mutations than patients with transmembrane (p = 0.005) or cytoplasmic (p = 0.026) mutations. No differences in progression slopes of I4e seeing areas were observed between affected domains (p = 0.233).

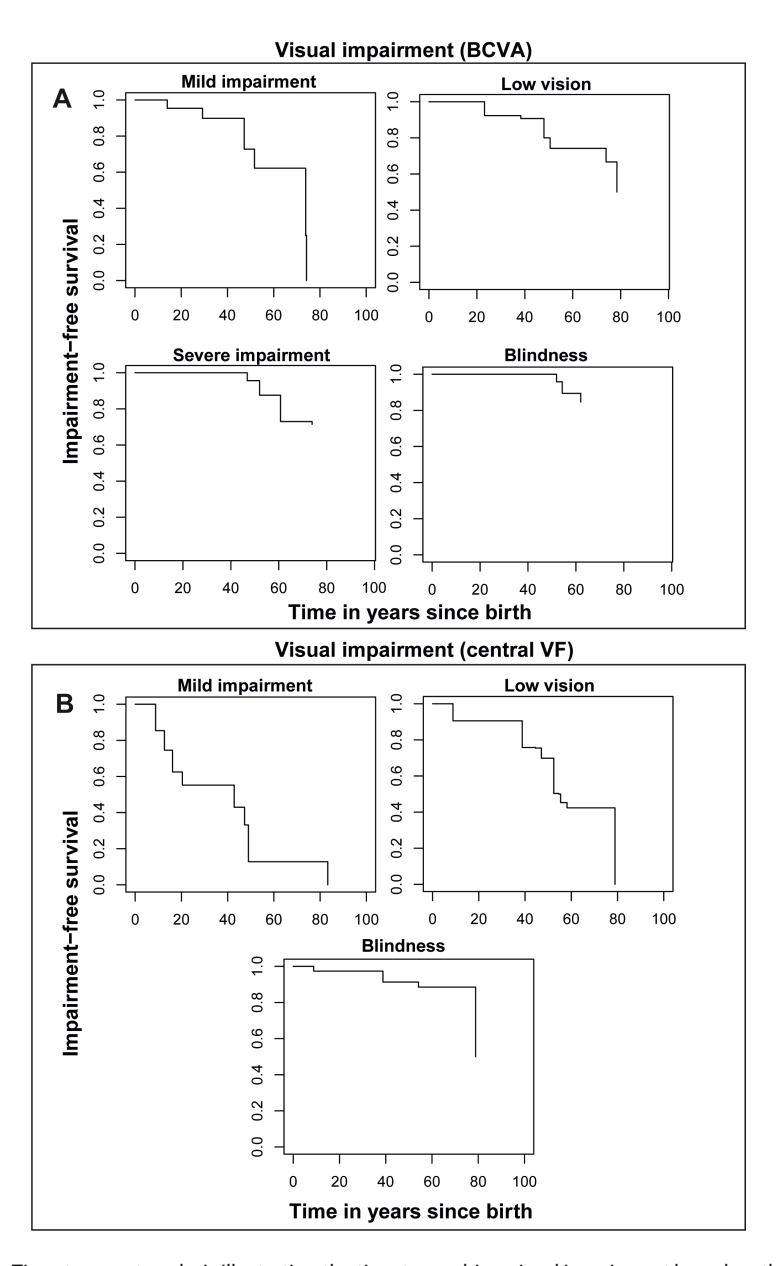


**Figure 2.** Time-to-event analysis illustrating the time to reaching visual impairment based on the definition set by the World Health Organization. Due to the presence of left, interval and right censored data to estimate the time to low vision, severe impairment and blindness, the nonparametric maximum likelihood estimator (NPMLE) was employed. **A.** Time-to-event analysis of the best-corrected visual acuity (BCVA) in the better-seeing eye demonstrating the time to reaching mild visual impairment ( $(20/67 \le BCVA < 20/40)$ , low vision ( $(20/200 \le BCVA < 20/67)$ ), severe visual impairment ( $(20/400 \le BCVA < 20/200)$ ) or blindness (BCVA < (20/400)). **B.** For central visual fields (central VF), the following endpoints were used: mild impairment ( $(20°60 \le BCVA < 20°60)$ ), low vision (central VF < (20°60)) and blindness (central VF < (20°60)).

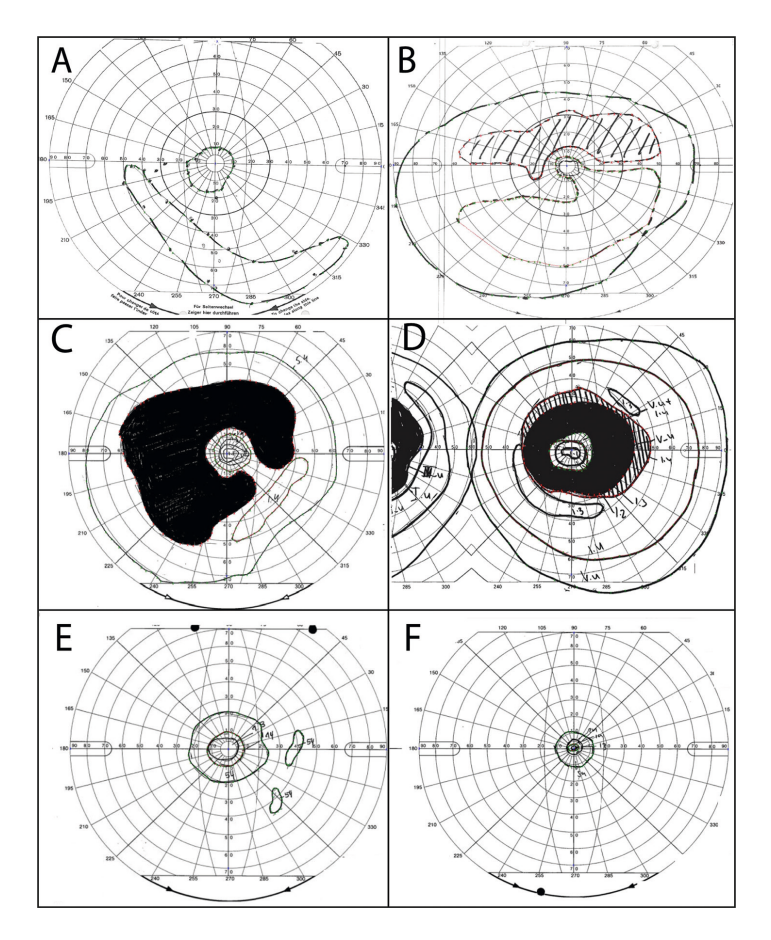


**Figure 3.** Representative patterns of visual field loss in patients with *RHO*-associated retinitis pigmentosa. **A-B**, intrafamilial variability in a family carrying the p.(Glu181Lys) mutation. **A**, Patient ID-30, aged 54 years, showed a central island with peripheral remnants (best-corrected visual acuity [BCVA] right eye: 20/100; BCVA left eye: 20/125) on kinetic perimetry, while the younger brother (**B**), aged 46 years, had an absolute scotoma in the superior hemifield (BCVA: 20/16 in both eyes). **C**, Patient-ID 52, aged 43 years, with the *RHO* missense mutation p.(Glu28His). An incomplete midperipheral annular scotoma was visible in the left eye (BCVA right eye: 20/25; BCVA left eye: 20/20). **D**, Patient-ID 39, aged 52 years, with a mutation c.937-2A>C (p.(?)) splice site mutation in *RHO*, showing a complete ring scotoma in the right eye (BCVA right eye: 20/67; BCVA left eye: 20/400). **E**, Patient-ID 59, aged 22 years, with *RHO* mutation p.Arg135Trp, showed severe constriction of the V4e and I4e isopters with central preservation of the visual field and small midperipheral visual field remnants (BCVA right eye: 20/67; BCVA left eye: 20/40). **F**, Patient-ID 44 (38 years of age), carrying the p.(Asp190Tyr) *RHO* mutation, had marked peripheral visual field loss with only a residual central island remaining (BCVA right eye: 20/50; BCVA left eye: 20/32).

#### Multimodal imaging

SD-OCT imaging was performed in 32 patients, with thickness measurements of retinal layers specified in Table 1. We found cystoid macular edema (CME) in 16 out of 32 patients (50%), which was located in the fovea for 12/16 (75%) patients.

No significant age effect was found on central retinal thickness (CRT) (p = 0.371) or ONL thickness (p = 0.502), after exclusion of patients with foveal CME. For PR+RPE measurements, advancing age was associated with the loss of PR+RPE thickness (-0.6%/year; p = 0.030), which was not affected by a sector RP phenotype (p = 0.611). The PR+RPE thickness was the only parameter, after exclusion of patients with foveal CME and correction for multiple testing, that correlated with BCVA (Table 2). The macular ellipsoid zone (EZ) band width, measurable in 26/32 (81%) patients, decreased with advancing age (-3.8%; p < 0.001), which was not significantly different in sector RP patients (p = 0.589). However, a larger EZ band width at baseline was seen in patients with a sector RP phenotype (p = 0.018). For generalized RP patients, no differences in the EZ band width at baseline (p = 0.185) or for the decline rates (p=0.886) were observed between affected protein domains. In 6/26 patients (23%), the EZ band width went beyond the scanning range on SD-OCT (Figure 4A). A granular interrupted aspect of the EZ band was seen in 9/26 (35%) patients.

FAF imaging, available for 38 patients, revealed hyper-autofluorescent (hyper-AF) and hypo-autofluorescent (hypo-AF) patterns in variable degrees, including a hyper-AF macular ring in 26/38 (68%) patients (Figure 4). In patients with sector RP, a common pattern seen on FAF was a hypo-AF distribution along the inferior vascular arcade, which corresponded with areas of degeneration seen on fundus photography (Figure 4D). A high degree of correlation was found between EZ band width and the horizontal ( $\rho$  = 0.923;  $\rho$  < 0.001), and vertical borders ( $\rho$  = 0.937;  $\rho$  < 0.001) of the hyper-AF macular ring.

**Table 2.** Structure and function correlations in *RHO*-associated retinitis pigmentosa.

	BCVA (logMAR)		Seeing retinal area V4e		Seeing retinal area l4e	
Visual function parameter	Spearman's rho	P-value	Spearman's rho	P-value	Spearman's rho	P-value
SD-OCT imaging						
CRT*	-0.370	0.095	0.291	0.274	0.086	0.770
ONL thickness*	-0.234	0.366	-0.029	0.923	-0.162	0.596
PR+RPE thickness*	-0.733	<0.001	0.528	0.053	0.556	0.049
EZ band width	-0.506	0.054	0.198	0.517	0.280	0.379
FAF imaging						
Horizontal ring diameter	-0.339	0.235	0.632	0.024	0.643	0.021
Vertical ring diameter	-0.245	0.419	0.615	0.037	0.566	0.059

The most recent mean values between right and left eyes were used for analysis. Imaging and measurements were performed using Heidelberg inbuilt software (Spectralis SD-OCT + HRA, Heidelberg Engineering, Heidelberg, Germany). Significance level was set at 0.003 following Bonferroni correction. Significant values are in bold. BCVA = best-corrected visual acuity. SD-OCT = spectral domain optical coherence tomography. EZ = ellipsoid zone. CRT = central retinal thickness. CRT = central retinal thi

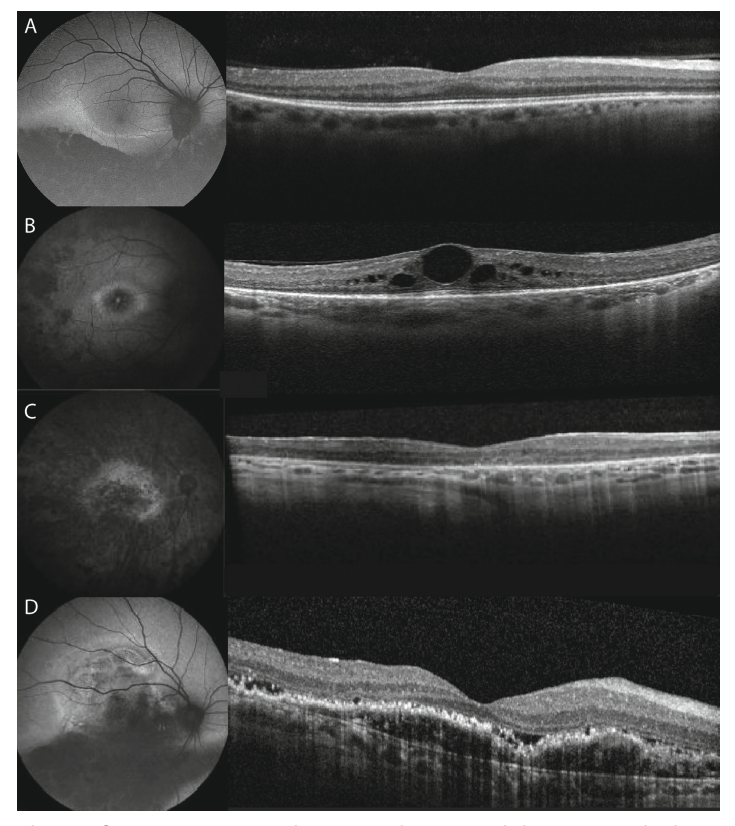


Figure 4. Fundus autofluorescence (FAF) and corresponding spectral-domain optical coherence tomography (SD-OCT) imaging in patients with RHO-associated retinitis pigmentosa. A, Patient-ID 81, aged 47 years, carrying the missense mutation p.(Asn15Ser). FAF imaging showed an inferior sectoral hypo-autofluorescence (hypo-AF), and ERG responses were reduced in a rod-cone pattern. SD-OCT imaging in this patient revealed central preservation of outer retinal layers, but with thinning of these layers in the peripheral macula. The ellipsoid zone (EZ) band width went beyond the scanning range nasally (best-corrected visual acuity [BCVA] right eye; 20/20; BCVA left eye; 20/22), B, Patient-ID 70, aged 26 years, with a p.(Glu181Lys) missense mutation. A well-demarcated hyper-autofluorescent (hyper-AF) ring was visible on FAF, with hypo-AF regions inside the hyper-AF ring. A small hyper-AF spot was seen at the foveal site, corresponding to the site of cystoid macular edema on SD-OCT. The midperipheral retina displayed normal AF regions surrounded by granular hypo-AF in variable intensities. Cystoid fluid collections were present in the inner and outer nuclear layer (BCVA right eye: 20/28; BCVA left eye, 20/33). C, Patient-ID 88, aged 60 years, carrying a p.(Pro347Leu) missense mutation in the RHO gene. FAF imaging reveals the near-absence of AF in the fovea and midperipheral retina, with residual AF remaining in the posterior pole. No evident hyper-AF ring is seen. Profound atrophy of all retinal layers is present on SD-OCT, with increased visibility of the underlying choroidal vessels. Granular remnants of the EZ are seen at the central fovea, but the EZ is completely absent in the peripheral macula (BCVA was 20/400 in both eyes). D, Patient-ID 80, aged 74 years, carrying the RHO missense mutation p.(Asn15Ser). FAF imaging showed sectorial degeneration hypo-AF along the inferior vascular arcade, corresponding with the RPE atrophy seen on fundus photography (Figure 1F). On SD-OCT, a pigment epithelial detachment was observed. The partly hyperreflective structures underlying the RPE detachment suggest presence of a neovascular membrane. The different layers of the neuroretina were still discernible, with a BCVA of 20/33 and 20/22 in the right and left eye, respectively.

#### DISCUSSION

This multicenter study provides a detailed description of the natural history of *RHO*-associated adRP, using cross-sectional and longitudinal data. We found a high prevalence of the p.(Gly181Lys) mutation (n=23), in 4 different families, accounting for 37% of the Dutch cohort. This mutations has rarely been described in other populations, which is suggestive of a founder effect of p.(Gly181Lys) in the Dutch *RHO*-associated adRP patients. Common mutations exclusively found in the Belgian patients of our cohort were p.(Ile255del) and p.(Tyr178Asp). The p.(Tyr178Asp) mutation has never been described outside the Belgian population, whereas the p.(Ile255del) mutation has previously been found in a single Irish family.<sup>19</sup>

Several mutations, such as the p.(Glu181Lys), found in this cohort could present as either generalized or sector RP, which underlines the potential influence of genetic and/or other modifiers on the phenotype. As suggested previously, it is possible that sector RP will eventually transition into a generalized RP phenotype in later stages of the disease.<sup>7</sup> However, we were not able to observe this transition in any of our patients. In addition, we found patients that retained a sector RP phenotype up to the 8<sup>th</sup> decade of life.

Our reported progression rates of BCVA (-3.8%/year) and V4e seeing areas (-5.6%/year) in patients with generalized RP were faster than those reported by a previous natural history study on *RHO*-associated RP, which reported rates of -1.8% per year for BCVA and -2.6% per year for V4e seeing areas.9 One possible explanation for this discrepancy is the difference in statistical methods. In contrast to the study of Berson and collaegues,9 we analyzed patients with a sector RP separately, as these patients demonstrated minimal disease progression and may contribute to a ceiling effect. Additionally, there are notable genetic differences between our population and the one in the American study by Berson and colleagues. The p.(Pro23His) mutation, which is the most common *RHO* mutation in the United States (36% in their cohort), is known to express a particularly mild phenotype, and is also described in patients with sector RP.<sup>20</sup> To the best of our knowledge, this founder mutation has never been reported in European studies, including the present one.<sup>21,22</sup>

Patients with a generalized form of RP were stratified based on the domains affected by RHO mutations. At baseline, we found larger EZ band widths on OCT and I4 seeing areas on GVF in patients carrying extracellular mutations, compared to patients with transmembrane or cytoplasmic mutations. No differences in annual decline rates of EZ band widths and I4e retinal seeing areas were found between mutated protein domains. In addition, mutations causing sector RP, showing minimal disease progression, were predominantly found in the extracellular domains. These findings support previous research in suggesting that extracellular mutations causes

milder phenotypes in *RHO*-associated RP.<sup>23-25</sup> The differences in disease expression between affected domains can be attributed to the biochemical defects caused by the mutations within these domains, although the role of external modifiers such as increased light exposure, especially in the development of sector RP, may also play a role.<sup>2,7</sup>

A limitation of this study is its retrospective nature, which limited a complete ascertainment of clinical data. ERG data were not available for all patients, and were mainly performed at baseline for diagnostic purposes. For this reason, a previously used classification system could not be applied to this cohort.<sup>10, 23, 24</sup> A prospective standardized natural history study on *RHO*-associated RP, which is currently unavailable to the best of our knowledge, should be able to address such limitations.

Pre-clinical studies on several gene knockdown and replacement strategies for *RHO*-associated RP have shown promising results, paving the way for human gene therapy trials.<sup>11, 12</sup> Our current clinical findings can have significant implications for future clinical treatment trials. We found a high degree of between-eye symmetry for all visual parameters (BCVA, V4e and I4e seeing retinal areas), supporting the use of the fellow eye as a control in intervention studies. On SD-OCT imaging, we found a high prevalence of CME, which may be a concern for future gene therapy trials, as the presence of CME may alter the retinal morphology, challenging correct injection of viral vectors into the subretinal space, and posing additional risks for per- and postoperative complications.<sup>26</sup> The borders of the hyper-AF ring on FAF imaging, which demarcates the transition zone between affected and unaffected retina,<sup>27</sup> correlated strongly with the EZ band width. FAF imaging should be used in conjunction with SD-OCT, in order to capture disease progression in less advanced stages of *RHO*-associated RP, in which the EZ band width can go beyond the 30° scanning range of SD-OCT (occurring in 23% of our cases).

The optimal intervention window for *RHO*-associated RP is before the 5<sup>th</sup> decade of life, as time-to-event analysis of visual fields revealed median ages of 52 and 79 for low vision and blindness, respectively. The use of visual acuity as an endpoint may be impractical for *RHO*-associated RP, due to the relatively late onset of BCVA-based impairment. Therefore, the use of surrogate endpoints for visual acuity could accelerate the measurement of disease progression and treatment response. We and others have previously found that the PR+RPE complex has been suggested to be a good predictor of visual acuity.<sup>15, 28-30</sup> Similar results were found in this study, as the PR+RPE complex correlated strongly with BCVA, and was the only parameter that remained significant after correction for multiple testing. The PR+RPE complex can potentially be used to identify early structural changes before visual acuity loss may be noticeable, which can be particularly useful in diseases with relatively slow disease progression such as *RHO*-associated RP. In anticipation of future clinical trials for *RHO*,

the establishment of potential clinical endpoints are necessary steps for an optimal study design. In this regard, this study highlights the potential use of the PR+RPE complex as a surrogate endpoint for BCVA in future clinical trials.

#### **ACKNOWLEDGEMENTS**

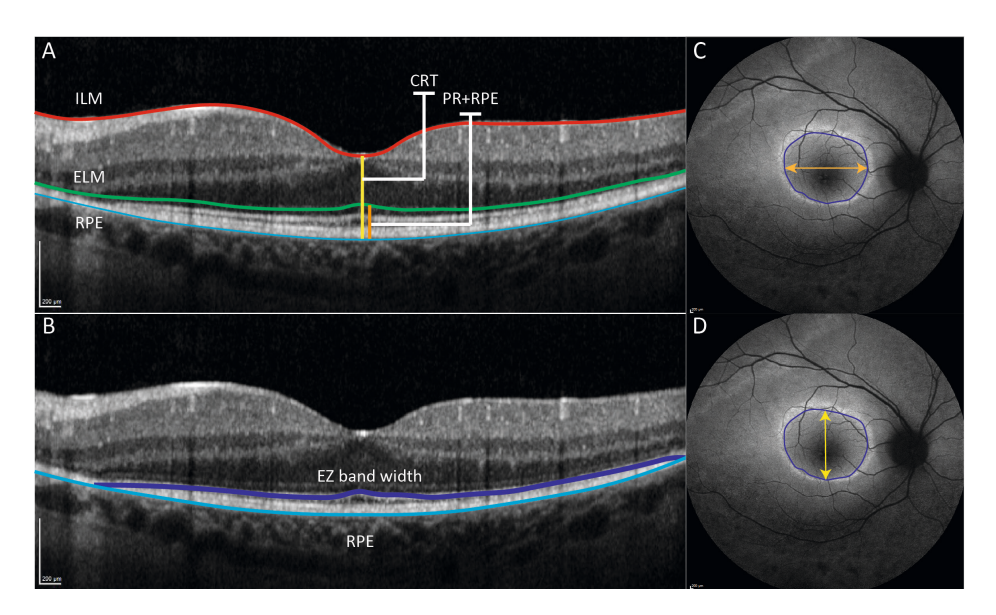
This study was performed as part of a collaboration within the European Reference Network for Rare Eye Diseases (ERN-EYE). ERN-EYE is co-funded by the Health Program of the European Union under the Framework Partnership Agreement #739543 – 'ERN-EYE' and co-funded by the Hôpitaux Universitaires de Strasbourg.

#### **RFFFRFNCFS**

- Dryja TP, Hahn LB, Cowley GS, et al. Mutation spectrum of the rhodopsin gene among patients with autosomal dominant retinitis pigmentosa. Proceedings of the National Academy of Sciences of the United States of America. 1991:88(20):9370-9374.
- 2. Verbakel SK, van Huet RAC, Boon CJF, et al. Non-syndromic retinitis pigmentosa. Progress in Retinal and Eve Research. 2018:66:157-186.
- 3. Zeitz C, Gross AK, Leifert D, et al. Identification and functional characterization of a novel rhodopsin mutation associated with autosomal dominant CSNB. Investigative Ophthalmology & Visual Science. 2008;49(9):4105-4114.
- 4. Comitato A, Di Salvo MT, Turchiano G, et al. Dominant and recessive mutations in rhodopsin activate different cell death pathways. Hum Mol Genet. 2016;25(13):2801-2812.
- Kranich H, Bartkowski S, Denton MJ, et al. Autosomal dominant 'sector' retinitis pigmentosa due to a point mutation predicting an Asn-15-Ser substitution of rhodopsin. Human Molecular Genetics. 1993;2(6):813-814.
- Berson EL, Rosner B, Sandberg MA, et al. Ocular findings in patients with autosomal dominant retinitis pigmentosa and a rhodopsin gene defect (pro-23-his). Archives of Ophthalmology. 1991;109(1):92-101.
- Ramon E, Cordomí A, Aguilà M, et al. Differential light-induced responses in sectorial inherited retinal degeneration. J Biol Chem. 2014;289(52):35918-35928.
- 8. Iannaccone A, Man D, Waseem N, et al. Retinitis pigmentosa associated with rhodopsin mutations: Correlation between phenotypic variability and molecular effects. Vision Research. 2006;46(27):4556-4567.
- 9. Berson EL, Rosner B, Weigel-DiFranco C, et al. Disease progression in patients with dominant retinitis pigmentosa and rhodopsin mutations. Investigative Ophthalmology & Visual Science. 2002;43(9):3027-3036.
- 10. Mendes HF, van der Spuy J, Chapple JP, et al. Mechanisms of cell death in rhodopsin retinitis pigmentosa: implications for therapy. Trends in Molecular Medicine.11(4):177-185.
- 11. Tsai Y-T, Wu W-H, Lee T-T, et al. Clustered regularly interspaced short palindromic repeats-based genome surgery for the treatment of autosomal dominant retinitis pigmentosa. Ophthalmology. 2018.
- 12. Cideciyan AV, Sudharsan R, Dufour VL, et al. Mutation-independent rhodopsin gene therapy by knockdown and replacement with a single AAV vector. Proceedings of the National Academy of Sciences. 2018;115(36):E8547.
- 13. van Huet RAC, Oomen CJ, Plomp AS, et al. The RD5000 Database: facilitating clinical, genetic, and therapeutic studies on inherited retinal diseases. Investigative Ophthalmology & Visual Science. 2014;55(11):7355-7360.
- 14. Dagnelie G. Technical note. Conversion of planimetric visual field data into solid angles and retinal areas. Clinical Vision Science. 1990;5(1):95-100.
- 15. Spaide RF, Curcio CA. Anatomical correlates to the bands seen in the outer retina by optical coherence tomography: literature review and model. Retina. 2011;31(8):1609-1619.
- 16. R: A language and environment for statistical computing [computer program]. Vienna, Austria: R Foundation for Statistical Computing; 2010.
- 17. Talib M, van Schooneveld MJ, Thiadens AA, et al. CLINICAL AND GENETIC CHARACTERISTICS OF MALE PATIENTS WITH RPGR-ASSOCIATED RETINAL DYSTROPHIES: A Long-Term Follow-up Study. RETINA. 2019;39(6):1186-1199.

- 18. Van Cauwenbergh C, Coppieters F, Roels D, et al. Mutations in splicing factor genes are a major cause of autosomal dominant retinitis pigmentosa in Belgian families. PLoS ONE. 2017;12(1):e0170038.
- 19. Inglehearn CF, Bashir R, Lester DH, et al. A 3-bp deletion in the rhodopsin gene in a family with autosomal dominant retinitis pigmentosa. American Journal of Human Genetics. 1991;48(1):26-30.
- 20. Oh KT, Weleber RG, Lotery A, et al. Description of a new mutation in rhodopsin, pro23ala, and comparison with electroretinographic and clinical characteristics of the pro23his mutation. Archives of Ophthalmology. 2000;118(9):1269-1276.
- 21. Blanco-Kelly F, García-Hoyos M, Cortón M, et al. Genotyping microarray: Mutation screening in Spanish families with autosomal dominant retinitis pigmentosa. Molecular Vision. 2012;18:1478-1483.
- 22. Audo I, Manes G, Mohand-Saïd S, et al. Spectrum of rhodopsin mutations in French autosomal dominant rod-cone dystrophy patients. Investigative Ophthalmology & Visual Science. 2010;51(7):3687-3700.
- 23. Cideciyan AV, Hood DC, Huang Y, et al. Disease sequence from mutant rhodopsin allele to rod and cone photoreceptor degeneration in man. Proceedings of the National Academy of Sciences of the United States of America. 1998;95(12):7103-7108.
- 24. Jacobson SG, McGuigan DB, Sumaroka A, et al. Complexity of the class B phenotype in autosomal dominant retinitis pigmentosa due to rhodopsin mutations. Investigative Ophthalmology & Visual Science. 2016:57(11):4847-4858.
- 25. Schuster A, Weisschuh N, Jägle H, et al. Novel rhodopsin mutations and genotype-phenotype correlation in patients with autosomal dominant retinitis pigmentosa. British Journal of Ophthalmology. 2005;89(10):1258.
- 26. Xue K, Groppe M, Salvetti AP, et al. Technique of retinal gene therapy: delivery of viral vector into the subretinal space. Eye. 2017;31(9):1308-1316.
- 27. Aizawa S, Mitamura Y, Hagiwara A, et al. Changes of fundus autofluorescence, photoreceptor inner and outer segment junction line, and visual function in patients with retinitis pigmentosa. Clinical & Experimental Ophthalmology. 2010;38(6):597-604.
- 28. Eliwa TF, Hussein MA, Zaki MA, et al. Outer retinal layer thickness as good visual predictor in patients with diabetic macular edema. RETINA. 2018;38(4).
- 29. Lim Jl, Tan O, Fawzi AA, et al. A pilot study of Fourier-domain optical coherence tomography of retinal dystrophy patients. American Journal of Ophthalmology. 2008;146(3):417-426.
- 30. Talib M, van Schooneveld MJ, Van Cauwenbergh C, et al. The Spectrum of Structural and Functional Abnormalities in Female Carriers of Pathogenic Variants in the RPGR Gene. Investigative Ophthalmology & Visual Science. 2018;59(10):4123-4133.

#### SUPPLEMENTAL CONTENT



**Supplementary Figure S1.** Measurement of structural layers and hyperautofluorescent foveal rings using the Heidelberg System (Spectralis SD-OCT + HRA, Heidelberg Engineering, Heidelberg, Germany). Errors in segmentation were corrected manually. (**A**) Measurement of the central retinal thickness (CRT), which was defined as the foveal thickness between the internal limiting membrane (ILM) and the retinal pigment epithelium (RPE) layer. Measurement of the photoreceptor-retinal pigment epithelium complex (PR+RPE), was defined as the foveal thickness between the external limiting membrane (ELM) and the basal border of the RPE layer. (**B**) The ellipsoid zone band width (dark blue) was followed nasally and temporally until it was indistinguishable from the retinal pigment epithelium (light blue). (**C-D**) On fundus autofluorescence imaging, the inner borders of the hyperautofluorescent ring were measured in the horizontal (C) and vertical axis (D) as illustrated.

**Supplemental Digital Content 2.** Cohort characteristics of Dutch and Belgian patients with *RHO*-associated dystrophies.

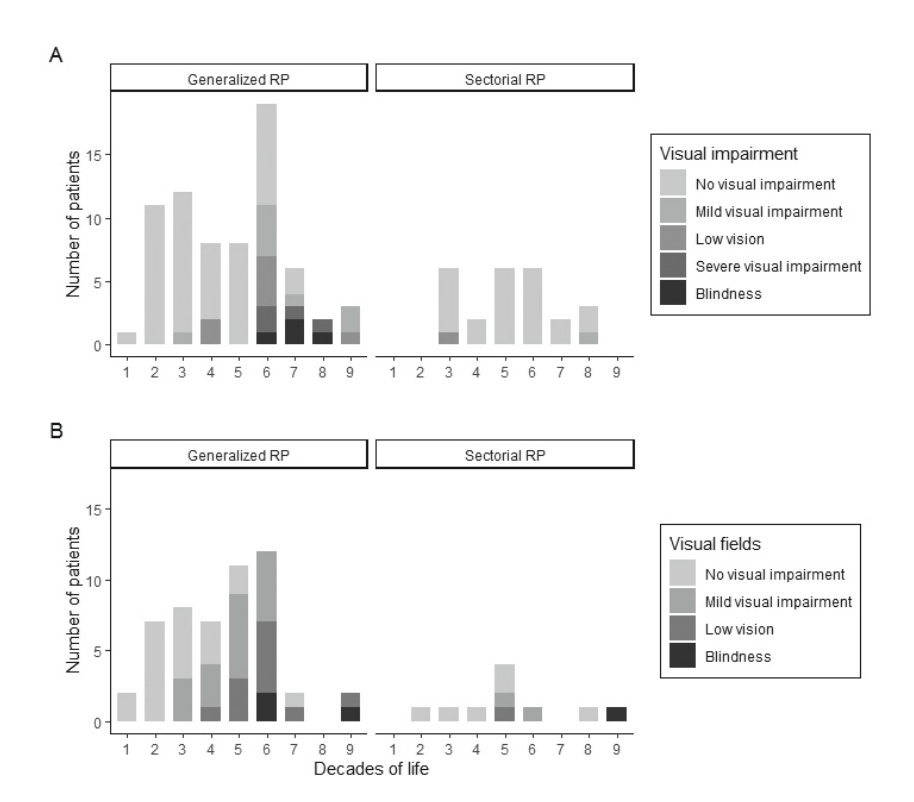
Characteristics	Total	Dutch patients	Belgian patients	P-value
Age at last examination	100	63	37	
(years), n				
Mean ± SD	43.5±18.5	44.6±18.3	41.6±18.7	0.426
Range	10.0-87.7	14.3-87.7	10.0-82.4	
Follow-up time (years), no.	72	44	28	
Median FU time (IQR)	6.9 (11.9)	6.8 (13.3)	6.9 (7.5)	0.238
Range	0.2-41.0	0.2-36.4	0.2-41.0	
BCVA at the last visit	95	61	34	
(decimals), n				
Median BCVA, Snellen (IQR)	20/25 (20/30)	20/25 (20/30)	20/27 (20/36)	0.368
Range	LP-20/12	20/1000-20/12	LP-20/20	
Seeing areas at last visit (I4e,	55	25	30	
mm²), n				
Median isopter size ( (IQR)	17.4 (101.4)	29.1	15.0	0.106
Range	0.8-667.8	1.2-667.8	0.8-292.5	
Seeing areas at last visit (V4e,	57	24	33	
mm²), n				
Median isopter size (IQR)	256.4 (545.6)	322.1 (547.5)	205.6 (545.6)	0.559
Range	4.0-764.9	14.5-763.9	3.7-764.9	

 $SD = standard\ deviation.\ FU = follow-up.\ BCVA = best-corrected\ visual\ acuity.\ IQR = interquartile\ range.\ LP = light\ perception.$ 

**Supplemental Digital Content 3.** Overview of mutations included in this study of *RHO*-associated retinitis pigmentosa.

Families affected	#	Nucleotide change	Amino acid change	Domain*	References
1	2	c.11C>A	p.(Thr4Lys)†	Extracellullar	Van den Born et al. 1994
3	4	c.44A>G	p.(Asn15Ser)†	Extracellullar	Yoshi et al. 1998
2	2	c.50C>T	p.(Thr17Met)†	Extracellullar	Dryja et al. 1991
2	2	c.68C>T	p.(Pro23Leu)†	Extracellullar	Dryja et al. 1991
3	8	c.84G>T	p.(Gln28His)†	Extracellullar	Fernandez al. 2014
1	1	c.119T>C	p.(Leu40Pro)	Transmembrane	De Sousa Dias et al. 2015
1	1	c.133T>C	p.(Phe45Leu)	Transmembrane	Dryja et al. 2000
1	3	c.265G>C	p.(Gly89Arg)	Transmembrane	Van Cauwenbergh et al. 2017
3	7	c.403C>T	p.(Arg135Trp)	Cytoplasmic	Jacobson et al 1991
1	4	c.512C>A	p.(Pro171GIn)	Transmembrane	Antiolo et al. 1994
1	6	c.532T>G	p.(Tyr178Asp)	Extracellullar	Van Cauwenbergh et al. 2017
1	1	c.538C>T	p.(Pro180Ser)	Extracellullar	Neveling et al. 2012
4	23	c.541G>A	p.(Glu181Lys)†	Extracellullar	Blanco-Kelly et al. 2012 Coussa et al. 2015
2	3	c.563G>A	p.(Gly188Glu)	Extracellullar	Macke et al. 1993
1	1	c.568G>A	p.(Asp190Asn)†	Extracellullar	Tsui et al. 2008
3	5	c.569A>G	p.(Asp190Gly)†	Extracellullar	Dryja et al. 1991
5	7	c.568G>T	p.(Asp190Tyr)	Extracellullar	Blanco-Kelly et al. 2012
1	1	c.641T>A	p.(Ile214Asn)†	Transmembrane	Neveling et al. 2012
1	1	c.759G>T	p.(Met253lle)	Transmembrane	Van Huet et al. 2015
1	6	c.763_765del	p.(Ile256del)	Transmembrane	Inglehearn et al. 1991
1	3	c.911T>A	p.(Val304Asp)	Transmembrane	Van Cauwenbergh et al. 2017
1	1	c.937-2A>C	Splice site	-	Novel
2	3	c.1028G>A	p.(Ser343Asn)	Cytoplasmic	Van Cauwenbergh et al. 2017
2	2	c.1033G>A	p.(Val345Met)	Cytoplasmic	Grøndahl al. 2006
3	3	c.1040C>T	p.(Pro347Leu)	Cytoplasmic	Blanco-Kelly et al. 2012 Dryja et al. 1990

 $<sup>\# =</sup> Frequency \ of \ affected \ individuals. \ RP = generalized \ retinitis \ pigmentosa. \ *Protein \ domain \ predicted \ to \ be affected \ by \ RHO \ mutations. \ ^tMutations \ associated \ with \ a \ sector \ RP \ phenotype.$ 



**Supplemental Digital Content 4.** Visual impairment in patients with *RHO*-associated retinitis pigmentosa (RP) by decades of life, classified as either generalized RP or sector RP. **A,** Visual impairment based on last available best-corrected-visual acuity (BCVA), based on the criteria of the World Health Organization (WHO): No visual impairment (BCVA  $\geq$  20/40), mild visual impairment (20/67  $\leq$  BCVA < 20/40), low vision (20/200  $\leq$  BCVA < 20/67), severe visual impairment (20/400  $\leq$  BCVA < 20/200) or blindness (BCVA < 20/400). **B,** For visual impairment based on last available central visual fields (central VF; V4e), the following endpoints were used: mild visual impairment (20°  $\leq$  central VF < 70°), low vision (central VF < 20°) and blindness (central VF < 10°).

2.